MSDE

PAPER

View Article Online
View Journal | View Issue

Cite this: *Mol. Syst. Des. Eng.*, 2024, **9**, 781

Liquid metal–polymer nano-microconjugations as an injectable and photo-activatable drug carrier†

Tomoka Hirose, Robin Rajan, Eijiro Miyako * and Kazuaki Matsumura *

Materials with distinct stimulus-responsive properties hold potential as carriers in next-generation drug delivery systems. In this study, we propose the design and characterisation of a carrier that can stably administer drugs, regardless of external conditions, through a two-step reaction achieved by creating a composite of materials possessing photothermal and temperature-responsive (dual-stimuli) characteristics. This composite, a novel integration of photothermal liquid metals (LMs) responsive to near-infrared laser irradiation and a temperature-responsive carboxylated polylysine-based polyampholyte, marks a significant advancement in drug delivery technology. The temperature-responsive liquid–liquid phase separation behaviour of the polymer, crucial for drug release, is precisely controlled by adjusting the ratio and concentration of the polymer anions and cations. Moreover, the heat required for phase separation and compatibility with the polymer solution is modulated through nanoparticle formation of the photothermal LMs, along with variations in the irradiation time and intensity of near-infrared laser light. Our findings, corroborated through laser microscopy and cell toxicity tests, demonstrate that this composite can generate heat upon photo-stimulation and use this heat to induce phase separation. Additionally, unlike conventional temperature-responsive carriers, this composite concentrates drugs, likely due to enhanced electrostatic interactions between the polyampholyte and the drug. This research not only overcomes the challenges faced by traditional stimulus-responsive carriers, which are influenced by the surrounding physiological environment, but also demonstrates the potential of a two-step reaction approach to concentrate and deliver drugs effectively.

Received 6th February 2024,
Accepted 30th April 2024

DOI: 10.1039/d4me00028e

rsc.li/molecular-engineering

Design, System, Application

Drug delivery systems (DDS) refer to a technology that delivers drugs to a target biological site in a time-dependent manner. Drugs, usually, lack the ability to target specific sites, thus requiring large dosages for eliciting the expected pharmacological effect. This can lead to significant side effects. Thus, DDS can be beneficial in targeted and effective delivery of drugs, such as anticancer agents. The design of an effective DDS is a subject of extensive research. Several biomaterials have been researched as DDS carriers and are designed to release drugs in response to a stimulus. However, interactions of these carriers with the complex physiological environment, may affect their ability to respond sensitively and promptly to the triggering stimulus. In this study, we have designed a carrier with two-step responsiveness, by creating a composite of materials with photothermal and temperature-responsive (dual-stimuli) characteristics. This composite is a novel integration of photothermal liquid metals responsive to near-infrared laser irradiation and a temperature-responsive carboxylated polylysine-based polyampholyte. It also shows a unique ability to concentrate drugs, during the temperature-responsive liquid–liquid phase separation and thus, holds promise as a highly effective next-generation DDS carrier.

1 Introduction

With the evolution of medical technology, the concept of drug delivery systems (DDS) with reduced side effects has gained traction in the field of drug discovery. DDS refers to a technology that delivers drugs to the appropriate biological site at the required time; various biomaterials have been researched as carriers for DDS.[1–7] Generally, drugs lack the ability to target specific sites, thus requiring consideration of absorption at sites other than the target site, for eliciting a pharmacological effect.[5,8] Thus, large drug dosages are often necessary, which can lead to significant side effects. The approach of DDS is of paramount importance, particularly for delivery of potent drugs such as anticancer agents.[9] Responsive polymers, which alter their properties in response to external stimuli, are among the most extensively studied

School of Materials Science, Japan Advanced Institute of Science and Technology, Asahidai, Nomi, Ishikawa 923-1292, Japan. E-mail: e-miyako@jaist.ac.jp, mkazuaki@jaist.ac.jp

† Electronic supplementary information (ESI) available. See DOI: https://doi.org/10.1039/d4me00028e

materials as carriers for DDS.[10] These materials can alter their properties and shapes in response to various stimuli such as changes in pH or temperature.[11–16] Typically, carriers are engineered to release or deliver drugs in response to a stimulus. However, due to the dynamic complexity of the biological environment, the ability to respond sensitively and promptly to the triggering stimuli is critical. Temperature-responsive polymers are one such type, changing properties such as solubility and shape in response to changes in temperature. While heat is easily supplied from external sources, it can be affected by the homeostasis of the biological system, necessitating precise design.

Poly(*N*-isopropylacrylamide) (PNIPAM)[17–21] is a representative temperature-responsive polymer that primarily exhibits a lower critical solution temperature (LCST)-type phase separation behaviour in aqueous solutions. Its phase separation temperature is close to that of the human body (30–32 °C), making it extensively studied as a biomaterial for DDS carriers and other applications. An increase in temperature causes a coil–globule transition; hence, since the phase separation temperature is strongly dependent on the composition of the polymer, it is necessary to synthesise polymers according to the temperature of the application environment.

Our group has previously reported a novel polyampholyte with new LCST-type phase separation characteristics by modifying the free amino groups in ε-poly-L-lysine (PLL), with succinic anhydride (SA), resulting in PLL–SA.[22,23] Compared to PNIPAM, the phase separation temperature of these polymers can be controlled by adjusting the polymer concentration without changing polymer composition. The phase separation temperature can be designed to range from 35–40 °C, which is more suitable for use as a thermoresponsive DDS carrier. Another advantage is that one of the raw materials, polylysine, is also used in food additives and has low cytotoxicity.[24] Interestingly, unlike typical LCST-type polymers, they can exhibit liquid–liquid phase separation and core–shell coacervation phenomena in the aqueous phase. Liquid–liquid phase separation is a phenomenon also observed within living organisms, driven by proteins and RNA, contributing to various metabolic processes within cells. In recent years, this behaviour has gained attention as a crucial element for deepening our understanding of life from the perspective of phase separation biology.[25]

Polyampholytes possess both anionic and cationic charges within the same molecule and are utilised in protein modelling, among other applications.[22,26–30] However, it is already known that PLL–SA does not exhibit phase separation in salt solution. This is because phase separation is driven by electrostatic interactions, which are neutralised in the presence of a salt solution. To be utilised as biomaterials, it is essential that phase separation remains stable even in salt solutions like bodily fluids. It has already been reported that the phase separation of temperature-responsive polymers such as PNIPAM and the polyampholytes under study, can be stabilised in salt-containing solvents by the introduction of hydrophobic moieties.

Therefore, in this study, we synthesised polymers in which carboxylation was achieved using phthalic anhydride (PA) which has aromatic rings and is known for its higher hydrophobicity than SA.[31] We evaluated the resulting polymer (PLL–PA). This modification ensures stable phase separation even in salt solutions, which is crucial for their use as biomaterials.

We hypothesised that the primary challenge associated with the application of temperature-responsive polymers in DDS, which is their high sensitivity to fluctuating thermal stimuli, could be effectively addressed by designing composite materials. These composites would integrate materials with diverse properties, enabling a self-regulating mechanism rather than relying on external control for drug delivery. Near-infrared light is appropriate as a source of heat generation by light stimulation because of its high penetration into living organisms and its use in medical practice. Therefore, materials with a photothermal effect on near-infrared light were applied in this study.

Many metallic nanoparticles have been reported as materials with photothermal effects, with gold nanoparticles being a typical example.[32] Gold nanoparticles absorb near-infrared light and are used as heat-generating materials in thermotherapy.[33–35] Metals such as gold and silver are characterised by their ability to produce particles with well-defined diameters[36] and allow easy surface modification. Liquid metals (LMs) are also a type of metal nanoparticles that show photothermal effect with near-infrared light.[37] Mercury, a typical LM, has several excellent mechanical properties, including high electrical conductivity and flexibility, but it is also known to have high biotoxicity. However, gallium-based LMs, which have been attracting attention in recent years, are chemically stable and have extremely low biotoxicity in addition to the properties of conventional LMs.[38–41] Furthermore, compared to other solid metals such as gold and silver nanoparticles, gallium-based LMs have a lower melting point, which makes it easier to break the oxide film formed on the metal surface and transform it into particles.[37,39,42] Particulation can also be achieved by a simple method such as sonication, which is ideal for processing composite materials.

The LM temperature-responsive polymer composite is a physical, stimulus-responsive carrier, triggered by light. In this study, the anticancer drug doxorubicin hydrochloride (DOX), was selected as the drug to be delivered, assuming that it is particularly suitable for anticancer drug therapy in spite of strong side effects. DOX is a widely used anticancer drug that inhibits DNA and RNA synthesis. Combined with near-infrared laser therapy, it is expected to exert its effects locally at the target site with minimal side effects.

Based on the above, the present study aimed to capitalise on the temperature-responsive attributes of the polyampholyte PLL–PA and harness the photofunctionality of LMs, to engineer a composite. This composite was designed

to exhibit a two-step responsive behaviour—a two-step stimuli-response—wherein stable heat generation, upon triggering with near-infrared laser light, induced phase separation. Through this approach, we endeavoured to fabricate, assess, and characterise an innovative, intelligent composite entity that exhibits a sequential response mechanism.

2 Experimental

2.1 Materials

A 25% PLL solution (with a molecular weight 4000 g mol^{-1} and degree of polymerization of 32) was procured from JNC Corporation (Tokyo, Japan). Anhydrous succinic acid and anhydrous phthalic acid were obtained from Nacalai Tesque Inc. (Kyoto, Japan). The powder form of phosphate-buffered saline (PBS (−)) was purchased from Shimadzu Diagnostics Corp. (Tokyo, Japan). The gallium–indium eutectic alloy was obtained from Alfa Aesar (Ward Hill, MA, USA). 2-Iminothiolane hydrochloride was procured from Toronto Research Chemicals Inc. (Toronto, Canada) and doxorubicin hydrochloride was procured from Wako (Osaka, Japan).

2.2 Synthesis of temperature-responsive polyampholytes

An aqueous solution of 25% PLL was prepared, and an appropriate amount of SA or PA was added to the solution. The mixture was stirred at 60 °C until complete dissolution of reagents. Fifty per cent of the amino groups of PLL carboxylated with SA or PA, were denoted as PLL–SA50 and PLL–PA50, respectively. To increase the affinity of PLL–PA with LM, 2-iminothiolane hydrochloride was added and the mixture was stirred at 25 °C for 1 h. In this process, 40% of the amino group of PLL was carboxylated with PA and 20% was thiolylated with 2-iminothiolane hydrochloride (PLL–PA–(SH)). The polymer solution obtained was lyophilised and stored under vacuum until use.

2.3 Characterisation of the polyampholyte polymers

The synthesised polymers were subjected to ^{1}H nuclear magnetic resonance (NMR) spectroscopy using a 400 MHz NMR instrument from Bruker. The NMR data acquired were analysed using the Topspin 3.6.5 software to calculate the compositional ratios based on the integration values.

The temperature responsiveness and phase separation temperature were determined using a temperature-controlled UV-vis spectrophotometer (UV-1800, Shimadzu Corp., Kyoto, Japan). Polymer solutions were placed in 2 mL quartz cells, and optical data were collected continuously at a fixed wavelength of 550 nm, while varying the temperature. The transmitted light intensity of the homogeneous solution state prior to phase separation was set as 100%, and the temperature at which the transmitted light intensity reached 50% was defined as the phase separation temperature.

2.4 Particle formation of LM

Particle formation of the LM was achieved through ultrasonic treatment. Changes in particle size were observed using a transmission electron microscope (TEM) (HF-7650, Hitachi High-Tech Corp., Tokyo, Japan) to assess the effects of processing time and thiol functionalisation. Microgrids (NS-C15, Stem, Tokyo, Japan) were utilised for the observations. A diluted sample solution was deposited onto the grid with a droplet, dried at 50 °C, washed with distilled water for salt removal, and subsequently dried again in an oven. The size of the nanoparticles was determined using the dynamic laser scattering (DLS) method and a Zetasizer 300 system (Malvern Instruments, Worcestershire, UK), which was equipped with a He–Ne laser with a wavelength of 633 nm and a scattering angle of 173°.

2.5 Characterisation of composites

Confirmation of the photothermal effect of the composite and verification of control were performed by irradiating 1 ml of sample solution in a cell with a laser beam with a wavelength of 785 nm (BRM-785-1.0-100-0.22-SMA; B&W Tek, Newark, DE, USA, 6.29 W cm^{-2}), taking thermographic (FLIR i7: FLIR Systems) images, and evaluating with a thermocouple thermometer (AD-5601A: A&D Company, Tokyo, Japan).

The two-step reaction was observed using a laser scanning microscope (IX73: Olympus, Tokyo, Japan), by placing a droplet of the sample solution on a glass slide, covering it with a coverslip, and irradiating it with 808 nm laser light for 3 s.

DOX dissolved in PBS was used as the solvent in the polymer solution preparation, and the composite sample was prepared by adding LM followed by sonication, as described previously. The sample solution was adjusted to phase separation at 41 °C, and the final concentration of DOX was calculated using a calibration curve.

The release rate of DOX was determined by irradiating a 1 mL sample solution in a cell with 808 nm laser light (LSR808-5W-FCH: LASEVER) for 3 min, to induce phase separation (15.3 W cm^{-2}). The concentrations of DOX in the upper and lower phases were calculated based on the calibration curve obtained, using a microplate reader (Infinite 200 PRO M Nano+: Tecan, Männedorf, Switzerland) at 480 nm.

2.6 Cell viability assay

To assess the functionality of the composites and the efficacy of drug action, a 3-(4,5-dimethylthiazol-2-yl)-2,5-diphenyltetrazolium bromide (MTT) assay was performed. The polymer concentration was adjusted and fixed at 25 wt% to achieve phase separation at 41 °C. Composites were prepared either containing DOX (1 μg mL^{-1}) or without DOX. Cytotoxicity was compared with and without laser irradiation (808 nm, 3 W, 5 min) (15.3 W cm^{-2}).

Human colon adenocarcinoma HT-29 cells (from DS Pharma Biomedical (Tokyo, Japan)) were cultured and 500 μL of cell suspension was added to 24-well plates at a density of 6000 cells per mL. After 60 h of incubation, the samples (500 μL) were added, followed by laser irradiation and continued incubation. After 3, 6, and 24 h, samples were removed, and residual samples were washed with PBS. Subsequently, MTT solution dissolved in DMEM without foetal bovine serum (FBS), at a concentration of 100 μg mL^{-1}, was added in 500 μL aliquots and incubated for 4 h. The liquid was then removed, and 500 μL of DMSO was added. To completely remove the LM, the solution obtained was transferred to microtubes and subjected to centrifugation (20 °C, 1000 rpm, 5 min), and the resulting supernatants were transferred to a 96-well plate, in 100 μL aliquots, for measurement using a microplate reader (λ = 540 nm).

2.7 Statistical analysis

All data are presented as the mean ± standard deviation (SD). All experiments were conducted in triplicate. A one-way ANOVA with *post hoc* Fisher's protected least significant difference test was used for comparison among groups. Differences were considered statistically significant at a $p < 0.05$.

3 Results and discussion

Temperature-responsive polyampholytes, PLL–SA and PLL–PA, were synthesised by adding SA and PA to a PLL solution, according to Scheme 1. The synthesis was performed under heating and stirring conditions, resulting in the formation of carboxylated polylysine solutions. Further synthesis of PLL–PA(–SH) involved the addition of 2-iminothiolane hydrochloride to the PLL–PA obtained, followed by 1 h of stirring at 25 °C. Degree of substitution was calculated from integration values using ^{1}H NMR spectroscopy (Fig. S1 and S2 and Table S1†).

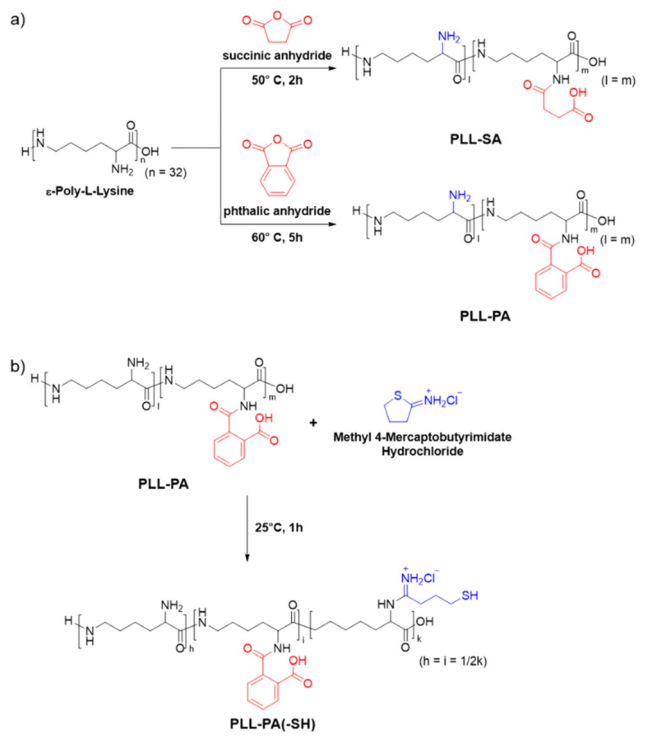

Scheme 1 Synthesis of (a) PLL–PA and (b) PLL–PA(–SH).

The introduction ratio of anions can be easily varied by adjusting the feeding amounts of SA and PA. In order to obtain phase separation temperatures relevant for biomaterial applications,[17,19] an introduction ratio in the range of 40–60% is considered suitable. When utilised as carriers in this study, polymers in a state where the ratio of anions (–COOH) to cations ($-NH_2$) was equimolar were synthesised and employed (for PLL–SA, PLL to SA ratio of 50 : 50; for PLL–PA, PLL to PA ratio of 50 : 50; and for PLL–PA(–SH), PLL to PA to SH ratio of 40 : 40 : 20).

To assess the temperature responsiveness of PLL–PA and PLL–PA(–SH) in both pure water and saline solution, we conducted measurements of transmitted light intensity using a temperature-variable UV-vis spectrophotometer. In case of PLL–SA50, phase separation was observed only in pure aqueous solution, as shown in Fig. 1(A); the phase separation temperatures for different concentrations of PLL–SA50 in pure water solvent were as follows: 3.2, 11 and 41 °C at 12, 12.5 and 15% polymer concentrations, respectively. No change in the transmitted light intensity was observed at any concentration with PBS as solvent. The phase separation temperatures at 12% and 15% polymer concentrations were 3.2 °C and 41 °C, respectively, indicating that phase separation can be induced over a wide range of temperatures by adjusting polymer concentration. In contrast, phase separation temperatures for different polymer concentrations of PLL–PA50 in pure water solvent were as follows: 11.5, 19 and 34 °C at 22.5, 25 and 30% polymer concentrations, respectively. In PBS solvent, the temperatures were 27.5, 37 and 50 °C at 20, 25, 30% polymer concentrations, respectively. PLL–PA exhibited phase separation in aqueous solution and PBS (Fig. 1(B)), suggesting that PLL–PA can be used over a wide temperature range by adjusting polymer concentration in the physiological salt environment. The same behaviour was confirmed for PLL–PA(–SH) (Fig. 1(C)). The phase separation temperature curves obtained from these experiments confirm the presence of LCST-type phase separation and demonstrate that the phase separation temperature can be tuned over a wide range by adjusting polymer concentration.

The phase-separation behaviour of PLL–PA and PLL–PA(–SH) in salt solutions is thought to be due to the π–π interactions caused by the introduction of the benzene ring.[23] We also confirmed that the phase separation temperature decreased at the same concentration, as more hydrophobic moieties were introduced, and the phase diagrams are depicted in Fig. S3.† This could be due to the fact that the main phase separation behaviour is caused by the electrostatic interaction between the amino and carboxyl

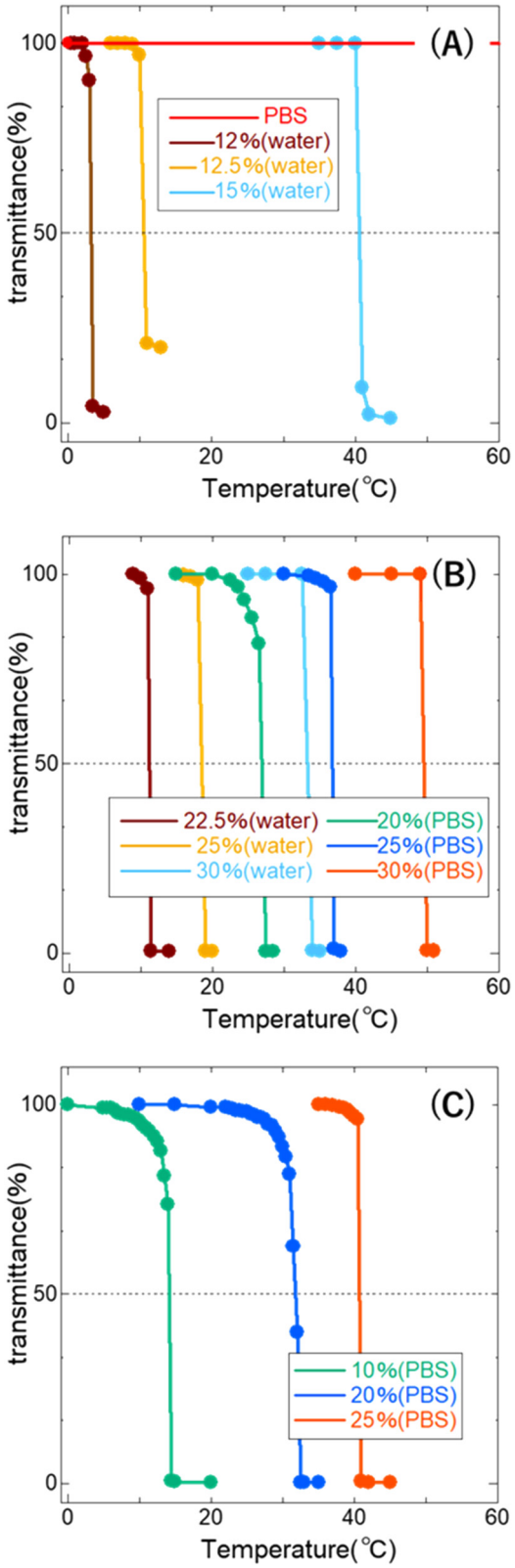

Fig. 1 Changes in transmittance intensity across different temperature ranges (UV-vis, λ = 550 nm; 50% transmittance indicates phase separation temperature). (A) The phase separation temperatures for different polymer concentrations of PLL–SA50 in pure water. (B) The phase separation temperatures for different polymer concentrations of PLL–PA50 in pure water and PBS. (C) The phase separation temperatures for PLL–PA(–SH) at various concentrations in PBS.

groups, whereas an excess of anionic carboxyl groups causes an imbalance in the interaction.[23]

These results confirm that PLL–PA50 and PLL–PA(–SH) are polyampholytes capable of stable phase separation at salt concentrations encountered in physiological conditions; this is necessary for temperature-responsive biomaterials.

With cancer treatment as the target application, we decided to employ PLL–PA(–SH) with a 25 wt% polymer concentration and a phase separation temperature of 41 °C as the designated DDS carrier. As the next step, we explored the optimal conditions for the particle formation of the LM, the other component of the composite. LM was added to a polymer solution (10 mL) adjusted to the optimal concentration, and variations in conditions were introduced through sonication. Pulsed sonication was chosen due to the simplicity of the method and uniformity in the particle size achieved during particle formation for composite preparation. The changes in particle size by sonication and the dispersion effect resulting from thiolation of the polymer were evaluated by TEM and DLS measurements of the composite after sonication with a 10-fold dilution (Fig. 2). Since heat generation during sonication in pulse mode,[43] can cause potential thermal damage to the polymer, a sonication time of 5–10 min was deemed appropriate in this study. However, for both sonication times, aggregation of LMNPs was observed more frequently with PLL–PA50 than without PLL–PA50.

The effect of thiolation on the polymer, to increase the affinity as a composite, was evaluated by preparing a similar sample using PLL–PA(–SH). Nanoparticles subjected to sonication in the presence of PLL–PA(–SH) for 5 minutes resulted in smaller particles compared to those sonicated in the presence of PLL–PA50 for the same time duration. Extending the treatment time to 10 minutes led to the

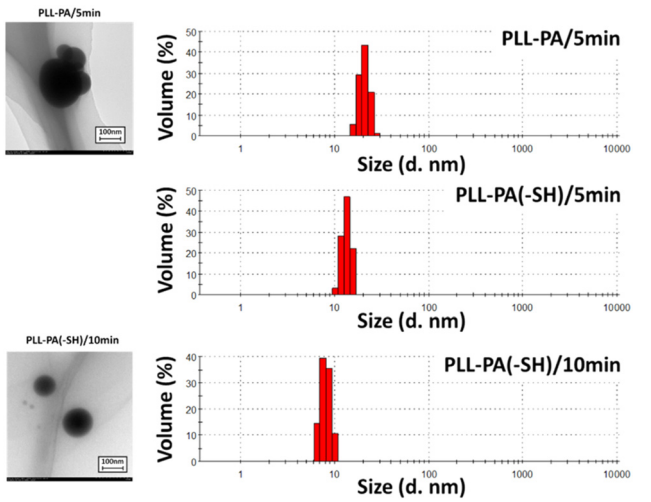

Fig. 2 TEM images and DLS measurements demonstrating LM nanoparticle formation and thiolation *via* pulse sonication with 2 s of irradiation per pulse (20 kHz, ice bath, 10 mL polymer solution, 30 μL LM).

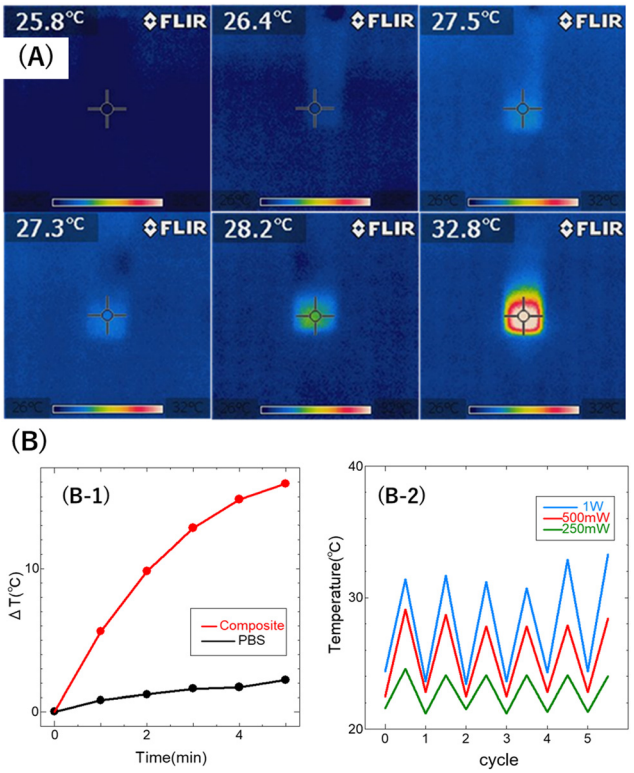

Fig. 3 Characterisation of the photo-thermal properties of the complex under near-infrared laser (λ = 785 nm) exposure: (A) thermography images: top row – PBS solution (1 mL), bottom row – complex (1 mL) at 0, 1 and 3 min of irradiation. (B) Temperature changes in samples (PBS or complex) in a 96-well plate measured *via* thermocouple: (B-1) temperature variations for both samples during irradiation, and (B-2) thermal cycling of the complex across 5 cycles at different power levels.

production of even smaller particles. The findings indicate that the addition of thiol groups improves the dispersibility of LMNPs, underscoring the benefits of thiolation in the preparation of the complex.

Following the assessment of the compatibility between the polymer and LM for use as a complex, we further characterised the complex as such. Exploration of the photo-thermal characteristics of the complex and its control was carried out through thermographic measurements (Fig. 3(A)) and thermal cycling (Fig. 3(B)).

The thermographic images in Fig. 3(A) show results of the composite being heated by irradiation with a near-infrared laser (λ = 785 nm). In the control PBS solution in the upper panel, the temperature increased by only 1.8 °C after 3 min of irradiation. However, the temperature of the composite solution increased by 5.5 °C after 3 min of irradiation.

In Fig. 3(B), a 96-well plate containing 100 μL each of PBS solution and complex, was irradiated with the same near-infrared laser for each well, and the change in temperature was recorded using a thermocouple thermometer. The rate of change in temperature at each elapsed time was measured (Fig. 3B-1). The analysis revealed a weak correlation between laser irradiation time and temperature increase rate in the PBS solution. However, a clear correlation was observed in the complex containing LM. Fig. 3B-2 shows the thermal cycles of repeated irradiation and cooling, for the complex irradiated with different laser outputs. The range of temperature rise in the cycles were 2.8 ± 0.12 °C, 5.6 ± 0.41 °C and 7.9 ± 0.62 °C, with laser outputs of 250, 500 and 1000 mW, respectively. The high reproducibility suggests that the durability of the material and temperature can be controlled by the power of the laser. These results collectively demonstrate the photo-thermal characteristics of the complex and effectiveness of laser output and irradiation time on control, and confirm the sufficient heat resistance of the material.

Next, we investigated if the polymer solution component could undergo liquid–liquid phase separation by utilising the heat generated through the photothermal characteristics as a carrier for DDS. Using laser microscopy, we observed the behaviour of the composite material in real-time during laser irradiation (Fig. 4 and ESI† Movies S1 and S2). For understanding the core–shell formation of the complex, we also studied samples involving the addition of LM to a thiol-bearing, 16-mercaptohexadecanoic acid (MHDA) solution, followed by ultrasonic treatment. While the MHDA solution exhibited slight changes around LMNPs due to laser irradiation, no further changes were observed. Conversely, in the case of the complex, a behaviour was distinctly observed as LMNPs generated heat in response to near-infrared laser light, triggering core–shell formation of the polymer solution around the particles, which then spread. As a result, we confirmed that the complex heated by near-infrared laser exhibited an increase in the overall temperature as the irradiation time was prolonged. The results from laser microscopy indicate the capability to capture the initial-stage changes of the complex.

Based on these observations, we confirmed that the complex possessed a two-step responsiveness, as intended,

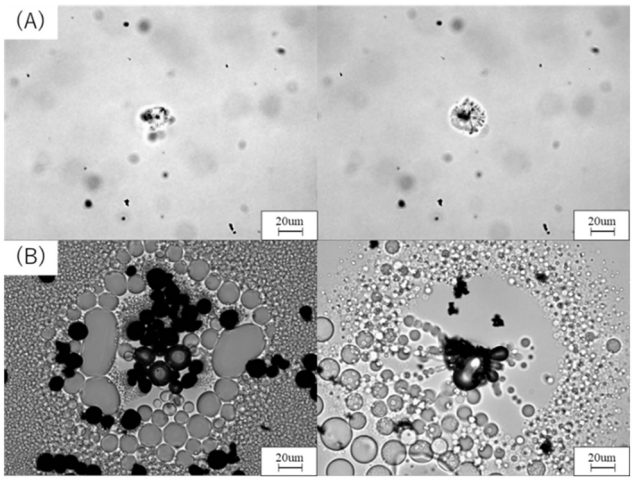

Fig. 4 Laser microscopy images (λ = 808 nm, irradiation: 3 s, scale: 20 μm): (A) MHDA + LMNPs solution, and (B) composite.

where it generates heat in response to light stimulation and utilises this heat to induce phase separation behaviour.

Following the confirmation of the desired properties of the composite, actual drug release experiments were conducted by adding the anticancer drug DOX, to the composite. The drug release rate was calculated by measuring three different states: the initial homogeneous state of the composite solution, the upper phase, and the lower phase after laser irradiation-induced phase separation, using a microplate reader. Due to the scattering effect caused by the presence of LMNPs, it was not feasible to directly measure the DOX concentration. Therefore, a polymer solution with an equivalent concentration to the composite without LM was prepared and measured for this purpose. Fig. 5 shows the sample after phase separation. Due to the intricate nature of the liquid–liquid phase separation behaviour exhibited by this sample, achieving a complete separation between the upper and lower phases proved to be challenging. Compared to the DOX concentration in the homogeneous sample before phase separation, the DOX concentration in the upper phase after phase separation was about 20%, while that in the lower phase was up to 150%.

From the aforementioned results, it was evident that the composite exhibited a behaviour where it concentrated the drug in the lower phase during phase separation, rather than releasing the drug upon phase separation. This characteristic is unique, differing from that of the conventional temperature-responsive carriers designed for drug-release. Furthermore, given the maximum concentration enhancement factor of 1.5, we deduced that this composite holds the potential to be a carrier with reduced side effects in drug delivery applications.

By enhancing the localised concentration of the drug at the intended site, this approach affords the potential to maximise therapeutic outcomes while minimising adverse reactions when employed as a DDS carrier.

Following the discovery of this capability of the complex to concentrate the drug from low concentrations for effective action, this function was evaluated for cytotoxicity using the MTT assay.

The composite was prepared at a polymer concentration of 25 wt/wt% (10 mL), an LM volume of 30 μL, and a DOX concentration of 1 μg mL^{-1} to demonstrate the phase separation temperature of 41 °C. Human colon adenocarcinoma HT29 cells were used for the experiment and seeded in 24-well plates at a density of 6000 cells per mL

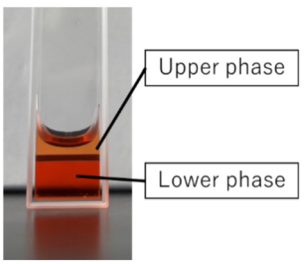

Fig. 5 Composite after phase separation.

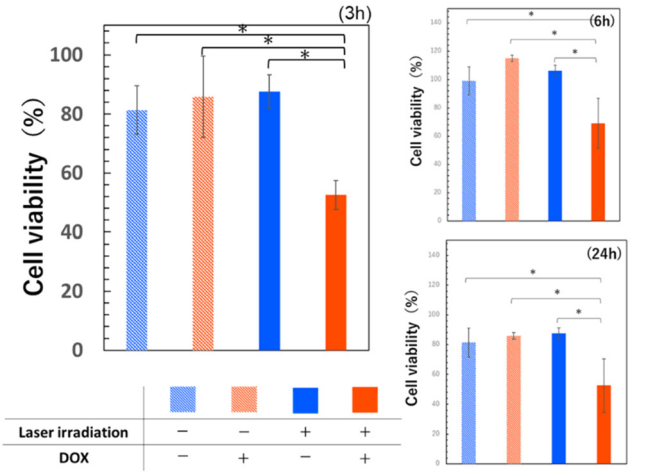

Fig. 6 Results of HT-29 cell viability using MTT assay. Errors bars indicate standard deviation of the mean. $p < 0.05$.

per well and employed for the assay after 2.5 days of incubation. Experimental groups were established, including groups with and without DOX, as well as groups with and without laser irradiation (Fig. 6).

For all observed time points, the group treated with laser irradiation using the composite with DOX, exhibited the lowest cell viability. The initial DOX concentration contained in the complex was 1 μg mL^{-1}, and the lower phase DOX concentration after phase separation is thought to be a maximum of 1.5 μg mL^{-1}, due to the concentration effect. The significant toxicity at this concentration is a result consistent with previous reports.[44] There was no significant difference in cell viability between the DOX-containing group without laser irradiation and the group without DOX, suggesting that the DOX concentration of 1 μg mL^{-1} employed in this experiment was a non-toxic, low concentration for cells. The effectively higher concentration after phase separation in the irradiated DOX group may have led to this result. Furthermore, the absence of a notable difference in cell viability regardless of laser irradiation in the DOX-free group indicated that the laser output used in this experiment did not exert a substantial impact on cell viability. It can therefore, be inferred that the lower cell viability observed only in the group treated with DOX-containing composite and laser irradiation, is attributed to the property of the composite, where photothermal stimulation induced by near-infrared laser light triggered heat generation and utilised this heat for phase separation and drug concentration.

From the results of the cell viability assays, we conclude that the composite exhibits the designed functionality and effectively exerts its intended action.

Conclusions

This study aimed to address the challenges in the application of conventional temperature-responsive polymers in DDS, by

utilising a composite consisting of a highly biocompatible near-infrared laser-responsive LM. The composite developed in this study is an intelligent material with two-step responsiveness, possessing the unique ability to concentrate drugs. We firmly believe that this composite is a highly effective and low side-effect next-generation DDS carrier.

The phase separation temperature required for drug-release can be readily adjusted through variations in polymer concentration, and the necessary heat can be controlled *via* the near-infrared laser light output and irradiation time. The designed composite demonstrates the anticipated photothermal characteristics triggered by light stimulation, inducing temperature-responsive liquid–liquid phase separation. Furthermore, unlike conventional carriers, the composite concentrates the drug during phase separation, further confirmed in the cytotoxicity test.

Although challenges remain in terms of precise control over LM particle size and the phase separation temperature dependence on polymer concentration, practical applications can be enhanced. By modulating parameters like ultrasonic treatment conditions and polymer concentration, the amphiphilic properties of these polymers can be leveraged to design optimal DDS carriers in forms such as gels and micelles.

Author contributions

T. H.: writing – original draft, methodology, investigation, visualization; R. R.: methodology, writing – review & editing; E. M.: conceptualization, methodology, supervision; K. M.: conceptualization, funding acquisition, methodology, project administration, resources, supervision, validation, writing – review & editing.

Conflicts of interest

There are no conflicts to declare.

Acknowledgements

This work was partially supported by Grants-in-Aid for Scientific Research (21H05516 (K. M.)) from the Japan Society for the Promotion of Science (JSPS).

References

1 T. Aziz, A. Ullah, A. Ali, M. Shabeer, M. N. Shah, F. Haq, M. Iqbal, R. Ullah and F. U. Khan, *J. Appl. Polym. Sci.*, 2022, **139**, e52624.
2 R. Langer, *Acc. Chem. Res.*, 2000, **33**, 94–101.
3 B. M. Holzapfel, J. C. Reichert, J. T. Schantz, U. Gbureck, L. Rackwitz, U. Nöth, F. Jakob, M. Rudert, J. Groll and D. W. Hutmacher, *Adv. Drug Delivery Rev.*, 2013, **65**, 581–603.
4 J. Liang, X. Peng, X. Zhou, J. Zou and L. Cheng, *Molecules*, 2020, **25**, 516.
5 C. Karavasili, D. A. Andreadis, O. L. Katsamenis, E. Panteris, P. Anastasiadou, Z. Kakazanis, V. Zoumpourlis, C. K. Markopoulou, S. Koutsopoulos, I. S. Vizirianakis and D. G. Fatouros, *Mol. Pharmaceutics*, 2019, **16**, 2326–2341.
6 M. Afshar, G. Dini, S. Vaezifar, M. Mehdikhani and B. Movahedi, *J. Drug Delivery Sci. Technol.*, 2020, **56**, 101530.
7 C. Orellana-Tavra, M. Köppen, A. Li, N. Stock and D. Fairen-Jimenez, *ACS Appl. Mater. Interfaces*, 2020, **12**, 5633–5641.
8 E. M. Pridgen, F. Alexis and O. C. Farokhzad, *Expert Opin. Drug Delivery*, 2015, **12**, 1459–1473.
9 O. Tacar, P. Sriamornsak and C. R. Dass, *J. Pharm. Pharmacol.*, 2013, **65**, 157–170.
10 K. Aoki and N. Saito, *Pharmaceutics*, 2020, **12**, 95.
11 J. Yan, X. Xu, J. Zhou, C. Liu, L. Zhang, D. Wang, F. Yang and H. Zhang, *ACS Appl. Bio Mater.*, 2020, **3**, 1216–1225.
12 D. Schmaljohann, *Adv. Drug Delivery Rev.*, 2006, **58**, 1655–1670.
13 M. Wei, Y. Gao, X. Li and M. J. Serpe, *Polym. Chem.*, 2017, **8**, 127–143.
14 A. K. Bajpai, S. K. Shukla, S. Bhanu and S. Kankane, *Prog. Polym. Sci.*, 2008, **33**, 1088–1118.
15 S. R. Sershen, S. L. Westcott, N. J. Halas and J. L. West, *J. Biomed. Mater. Res.*, 2000, **51**, 293–298.
16 A. Chilkoti, M. R. Dreher, D. E. Meyer and D. Raucher, *Adv. Drug Delivery Rev.*, 2002, **54**, 613–630.
17 K. Jain, R. Vedarajan, M. Watanabe, M. Ishikiriyama and N. Matsumi, *Polym. Chem.*, 2015, **6**, 6819–6825.
18 M. Heskins and J. E. Guillet, *J. Macromol. Sci., Part A: Pure Appl. Chem.*, 1968, **2**, 1441–1455.
19 M. Ebara, M. Yamato, T. Aoyagi, A. Kikuchi, K. Sakai and T. Okano, *Biomacromolecules*, 2004, **5**, 505–510.
20 T. Okano, N. Yamada, M. Okuhara, H. Sakai and Y. Sakurai, *Biomaterials*, 1995, **16**, 297–303.
21 F. A. Plamper, M. Ruppel, A. Schmalz, O. Borisov, M. Ballauff and A. H. E. Müller, *Macromolecules*, 2007, **40**, 8361–8366.
22 K. Matsumura, J. Y. Bae and S. H. Hyon, *Cell Transplant.*, 2010, **19**, 691–699.
23 E. Das and K. Matsumura, *J. Polym. Sci., Part A: Polym. Chem.*, 2017, **55**, 876–884.
24 C. Shi, Y. He, X. Feng and D. Fu, *J. Biomater. Sci., Polym. Ed.*, 2015, **26**, 1343–1356.
25 A. A. Hyman, C. A. Weber and F. Jülicher, *Annu. Rev. Cell Dev. Biol.*, 2014, **30**, 39–58.
26 K. M. Zurick and M. Bernards, *J. Appl. Polym. Sci.*, 2014, **131**, 40069.
27 K. Matsumura and S. H. Hyon, *Biomaterials*, 2009, **30**, 4842–4849.
28 R. Rajan, S. Ahmed, N. Sharma, N. Kumar, A. Debas and K. Matsumura, *Mater. Adv.*, 2021, **2**, 1139–1176.
29 K. Matsumura, F. Hayashi, T. Nagashima, R. Rajan and S. H. Hyon, *Commun. Mater.*, 2021, **2**, 15.
30 K. Matsumura, R. Rajan and S. Ahmed, *Polym. J.*, 2023, **55**, 105–115.
31 R. Rajan, N. Pangkom and K. Matsumura, in *ACS Symposium Series*, American Chemical Society, 2020, vol. 1350, pp. 47–62.

32 R. Sardar, A. M. Funston, P. Mulvaney and R. W. Murray, *Langmuir*, 2009, **25**, 13840–13851.
33 Z. Qin and J. C. Bischof, *Chem. Soc. Rev.*, 2012, **41**, 1191–1217.
34 H. Daraee, A. Eatemadi, E. Abbasi, S. F. Aval, M. Kouhi and A. Akbarzadeh, *Artif. Cells, Nanomed., Biotechnol.*, 2016, **44**, 410–422.
35 J. Lee, D. K. Chatterjee, M. H. Lee and S. Krishnan, *Cancer Lett.*, 2014, **347**, 46–53.
36 W. Haiss, N. T. K. Thanh, J. Aveyard and D. G. Fernig, *Anal. Chem.*, 2007, **79**, 4215–4221.
37 J. Ma, Y. Lin, Y. W. Kim, Y. Ko, J. Kim, K. H. Oh, J. Y. Sun, C. B. Gorman, M. A. Voinov, A. I. Smirnov, J. Genzer and M. D. Dickey, *ACS Macro Lett.*, 2019, **8**, 1522–1527.
38 S. A. Chechetka, Y. Yu, X. Zhen, M. Pramanik, K. Pu and E. Miyako, *Nat. Commun.*, 2017, **8**, 15432.
39 Y. Lu, Q. Hu, Y. Lin, D. B. Pacardo, C. Wang, W. Sun, F. S. Ligler, M. D. Dickey and Z. Gu, *Nat. Commun.*, 2015, **6**, 10066.
40 Y. Yu and E. Miyako, *iScience*, 2018, **3**, 134–148.
41 Y. Yu and E. Miyako, *Angew. Chem., Int. Ed.*, 2017, **56**, 13606–13611.
42 Y. Lin, Y. Liu, J. Genzer and M. D. Dickey, *Chem. Sci.*, 2017, **8**, 3832–3837.
43 A. Asadi, F. Pourfattah, I. Miklós Szilágyi, M. Afrand, G. Żyła, H. Seon Ahn, S. Wongwises, H. Minh Nguyen, A. Arabkoohsar and O. Mahian, *Ultrason. Sonochem.*, 2019, **58**, 104701.
44 R. Lüpertz, W. Wätjen, R. Kahl and Y. Chovolou, *Toxicology*, 2010, **271**, 115–121.